

Convection in rotating non-uniformly stratified spherical fluid shells: a systematic parameter study

Ján ŠIMKANIN¹, Pavel HEJDA¹, Dana JANKOVIČOVÁ²

¹ Institute of Geophysics, Academy of Sciences of the Czech Republic
Boční II/1401, 141 31 Prague, Czech Republic, e-mail: jano@ig.cas.cz, ph@ig.cas.cz

² Institute of Atmospheric Physics, Academy of Sciences of the Czech Republic
Boční II/1401, 141 31 Prague, Czech Republic, e-mail: dja@ufa.cas.cz

Abstract: A systematic parameter study of rotating convection in non-uniformly stratified spherical shells in dependence on the Prandtl number, Ekman number and Rayleigh number is presented. Attention is focused on the case, in which the thickness of both sublayers (stable and unstable) is the same (which was not investigated before). In our case the convection is not suppressed in the stably stratified region but, it is developed in both sublayers. Cases of small and large Prandtl numbers are characterized by the creation of multilayer convective structures. Convective motions take place simultaneously in the stable and unstable layers and form a multilayer structure. On the other hand, it is not possible to observe any multilayer convection for Prandtl number equal to one but it is possible to observe the small-scale structures. A conclusion is that our case is similar to the case in which the thickness of unstable sublayer is greater than that of stable one.

Key words: rotating convection, non-uniform stratification, control volume method, multilayer convection

1. Introduction

The Earth's and planetary fluid interiors are characterized by convective motions. Convection (magnetoconvection) constitutes the driving mechanism of hydromagnetic processes leading to magnetic field generation (*Roberts and Glatzmaier, 2000*). Buoyancy, the fundamental source of convection (magnetoconvection) (*Jones, 2000*), results from the complicated processes taking place in the Earth's and planetary fluid interiors, for example, a chemical homogenisation, gravitational differentiation, solidification processes acting on the inner core boundary (e.g., the convection in the mushy

layer due to the mentioned solidification processes, see *Guba and Woster (2006)*, etc. Consequently, the outer liquid Earth's core and the liquid interiors of Giant planets are non-uniformly stratified in density (see, *Fearn and Loper, 1981* and *Zhang and Schubert, 2000*).

It is assumed that the upper part of the outer liquid Earth's core (close to the core–mantle boundary¹) is stably stratified (subadiabatic radial temperature gradient) and the lower part (towards the inner core boundary²) unstably stratified (superadiabatic radial temperature gradient). Models of a non-uniformly stratified fluid shell (and also horizontal layer) are an acceptable simplification of the real Earth-like conditions. The stably stratified sublayer in the Earth's core is probably very thin, while the outer Earth's core is almost unstably stratified (see, *Fearn and Loper, 1981*; *Zhang and Schubert, 2000*; *Šimkanin et al., 2003* and *Šimkanin et al., 2006*). Such a stratification is probably typical for the terrestrial planets. However, in the other planets the ratio of the thickness of the appropriate sublayers (e.g., of the stably stratified to unstably stratified sublayers) and their geometric configuration vary. This is noticeable especially in the Giant planets (*Stanley and Bloxham, 2004*; *Stanley and Bloxham, 2006* and *Zhang and Schubert, 2000*).

Non-uniform stratification can be simulated thermodynamically also in the Boussinesq models by means of internal heat sources (*Zhang and Schubert, 2000*; *Šimkanin et al., 2003* and *Šimkanin et al., 2006*). If the stably stratified sublayer is very thin (for a stable/unstable geometric configuration), then the behaviour is close to the case of uniform stratification when the whole layer is unstably stratified. Likewise, if the unstably stratified sublayer is very thin, then the behaviour is close to the case of uniform stratification when the whole layer is stably stratified. Thus, the effects of non-uniform stratification are noticeable if the thicknesses of the stably and unstably stratified sublayers are comparable *Zhang and Schubert (2000)*, *Šimkanin et al. (2003)* and *Šimkanin et al. (2006)*, *Šimkanin (2008)*.

The study of hydromagnetic dynamo action in Mercury provides another good example of the influence of a stably stratified sublayer (*Christensen, 2006*). Mercury is characterized by a weak magnetic field. A possible explanation could be given by a hydromagnetic dynamo working in the similar

¹ hereinafter referred to as CMB

² hereinafter referred to as ICB

geometric configuration as in our study (stable/unstable), but in this case a larger fraction of the spherical shell is stably stratified (*Christensen, 2006*). In such a case the (magneto)convection and the dynamo action are strongly suppressed in the upper stably stratified sublayer, i.e. magneto(convection) and dynamo run in the small unstably stratified sublayer (close to ICB). Such weak dynamo action and skin-effect (the magnetic field generated in the unstably stratified sublayer permeates through the stably stratified sublayer where it is damped due to skin-effect) lead to the weak magnetic field observed on the surface of Mercury (*Christensen, 2006*).

For a different geometric configuration the influence of a non-uniform stratification is fundamental *Stanley and Bloxham (2004)*, *Stanley and Bloxham (2006)*. They assumed reverse stratification, i.e. the stably stratified sublayer is surrounded by the unstably stratified one. This configuration leads to non-dipolar and non-axisymmetric magnetic fields, which are typical e.g., for Uranus and Neptune.

The case, in which the thickness of both sublayers is the same, was not investigated in previous studies (e.g. *Zhang and Schubert, 2000*; *Šimkanin et al., 2003*; *Šimkanin et al., 2006*; *Šimkanin, 2008*). Consequently, we placed the change of the sign to the middle of the convective shell. A systematic parameter study of a convection in rotating non-uniformly stratified spherical fluid shells was performed. The model and governing equations are given in Section 2. The numerical results are presented in Section 3. Finally, Section 4 provides the conclusions.

2. Governing equations and model

Convection (with the velocity \mathbf{V}) of incompressible fluid in the Boussinesq approximation in a non-uniformly stratified spherical shell ($r_i < r < r_o$) rotating with angular velocity Ω is described by the system of dimensionless equations:

$$P_r^{-1} E \left(\frac{\partial \mathbf{V}}{\partial t} + (\mathbf{V} \cdot \nabla) \mathbf{V} \right) = -\nabla P - \mathbf{1}_z \times \mathbf{V} + R_a T r \mathbf{1}_r + E \nabla^2 \mathbf{V}, \quad (1)$$

$$\frac{\partial T}{\partial t} + (\mathbf{V} \cdot \nabla) T = \nabla^2 T + G(r), \quad (2)$$

$$\nabla \cdot \mathbf{V} = 0. \quad (3)$$

The typical length scale is the radius of the outer sphere L , which makes the dimensionless radius $r_o = 1$; the inner core radius r_i is similar to that of the Earth, equal to 0.35. (r, θ, φ) is the spherical system of coordinates, $\mathbf{1}_z$ and $\mathbf{1}_r$ are the unit vectors. The typical time t is measured in the unit of L^2/κ , typical velocity \mathbf{V} in κ/L and pressure P in $\rho\kappa^2/L^2$. The dimensionless parameters appearing in Eqs. (1–3) are the Prandtl number $P_r = \nu/\kappa$, the Ekman number $E = \nu/2\Omega L^2$ and the modified Rayleigh number $R_a = \alpha g_0 \delta T L / 2\Omega \kappa$, where κ is thermal diffusivity, ν is the kinematic viscosity, ρ is the density, α is the coefficient of thermal expansion, δT is the drop of temperature through the shell and g_0 is the gravity acceleration at $r = r_o$.

Equations (1–3) are closed by the non-penetrating and no-slip boundary conditions for the velocity field at the rigid surfaces and zero boundary conditions for temperature perturbations T .

The last term in Eq. (2), $G(r)$, constitutes the internal heat sources, which enable thermodynamically simulating the various stratifications of the spherical shells also in the Boussinesq models. The outer sphere was assumed to be stratified non-uniformly (it is divided into stably and unstably stratified sub-shells) with constant temperature $T_i = 1$ and $T_o = 0$ at the inner and outer boundaries of the shell, respectively. Thus, the non-uniform stratification due to internal heat sources was considered in the form:

$$G(r) = (9rr_i^2 - 12r + 6r^2r_i^2 + 60r^2 - 2r_i^2 - 8 + r_i^4 - 12r_i r^2 - 6rr_i^3 - 18r_i r) / [r(r_i^2 - 4)]. \quad (4)$$

$\partial T / \partial r$ changes its sign in the middle of the convective shell, $r_m = (r_i + r_o)/2$. Consequently, the width of both sub-shells is the same (more detailed description of $G(r)$, which is equivalent to the solution of Eq. (3) for the basic state ($\nabla^2 T + G(r) = 0$) with $T_i = 1$, $T_o = 0$ and $\partial T / \partial r = 0$ in r_m , is provided in *Reshetnyak and Steffen, 2005*).

3. Numerical results

Equations (1–3) were solved using the control volume method (*Hejda and Reshetnyak, 2003; Harder and Hansen, 2005*). The basic strategy of the method is to express the differential equations in conservative form, integrate them over the control volumes and convert every such integral into

the sum of fluxes over the boundary faces by means of Gauss' theorem (*Patankar, 1980*).

Our control volume code was validated against the so-called numerical dynamo benchmark (*Christensen et al., 2001*). Case 0 (the thermal convection in a rotating spherical shell) was successfully benchmarked and presented in *Hejda and Reshetnyak (2004)* and Case 2 (the dynamo with conducting and rotating inner core) in *Šimkanin and Hejda (2009)*. Parallelization is carried out using the message-passing interface (MPI). The computations were performed on an IBM Regatta p690+ cluster of SMP nodes in the John von Neumann Institute for Computing, Jülich Research Centre; the Sun Grid Engine at the Institute of Physics, Academy of Sciences of CR, Prague; the Nemo cluster (SGI) and PC clusters at the Institute of Geophysics, Academy of Sciences of CR, Prague.

As stated above, the outer Earth's core is probably non-uniformly stratified. The upper sublayer (close to CMB) is stably stratified ($\frac{\partial T}{\partial r} > 0$) and the lower one (close to ICB) unstably stratified ($\frac{\partial T}{\partial r} < 0$). We focused our attention to the case when the thickness of both sublayers is the same. This case was not investigated in previous studies by *Zhang and Schubert (2000)*, *Šimkanin et al. (2003)*, *Šimkanin et al. (2006)*, *Šimkanin (2008)*. Consequently, the change of the sign was placed to the middle of the convective shell.

The dependence of solutions on various values of the Prandtl number, P_r , the Ekman number, E , and the Rayleigh number, R_a , was investigated. Computations started from zero initial velocity and were performed for $P_r = 10^{-5}, 10^{-3}, 1, 10$; $E = 10^{-3}, 10^{-5}, 10^{-7}$ and $R_a \in \langle 10^2; 5 \times 10^5 \rangle$. The Prandtl number, the ratio of the thermal diffusion time to the viscous one, is the most significant dynamic factor in our study. According to the value of P_r it is possible to split the solutions to three qualitatively different groups, i.e. convection at low Prandtl numbers, at $P_r = 1$ and at large Prandtl numbers.

3.1. Low Prandtl numbers

In the case of low Prandtl numbers ($P_r < 1$ or $P_r \ll 1$) the characteristic thermal diffusion time is smaller (or much smaller) than the characteristic viscous diffusion time ($\tau_\kappa < \tau_\nu$ or $\tau_\kappa \ll \tau_\nu$), i.e. thermal diffusion pro-

cesses dominate over viscous ones. Inertial modes become important (see left side of Eq. (1), where the inertial term is not negligible in comparison with the viscous one). The monitored output parameters are the mean kinetic energy E_k and the mean angular drift of the solution ω (a solution drifts slowly with angular frequency ω in longitude). Their dependencies on the Rayleigh numbers R_a and the Ekman numbers E for $P_r = 10^{-5}$ and $P_r = 10^{-3}$ are given in Fig. 1. It is obvious that E_k and ω increase for

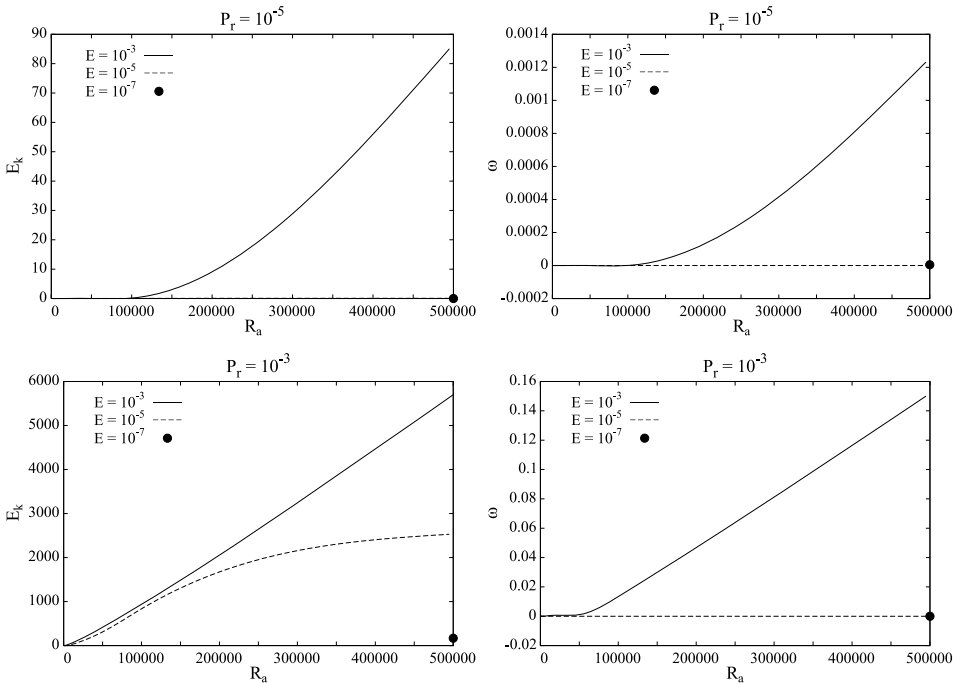


Fig. 1. Dependence of the mean kinetic energy E_k (left column) and the mean angular drift frequency ω (right column) on the Rayleigh number R_a and the Ekman number E for $P_r = 10^{-5}$ (top) and $P_r = 10^{-3}$ (bottom).

given E with the increase of R_a . Both E_k and ω decrease with the decrease of E . These features are well-known. In Fig. 1, E_k and ω for small values of E are always non-zero (they are too small compared to higher values of E). The cases $E = 10^{-3}$ and 10^{-5} were investigated and presented in many previous analyses. Consequently, we focused on the case $E = 10^{-7}$ (marked

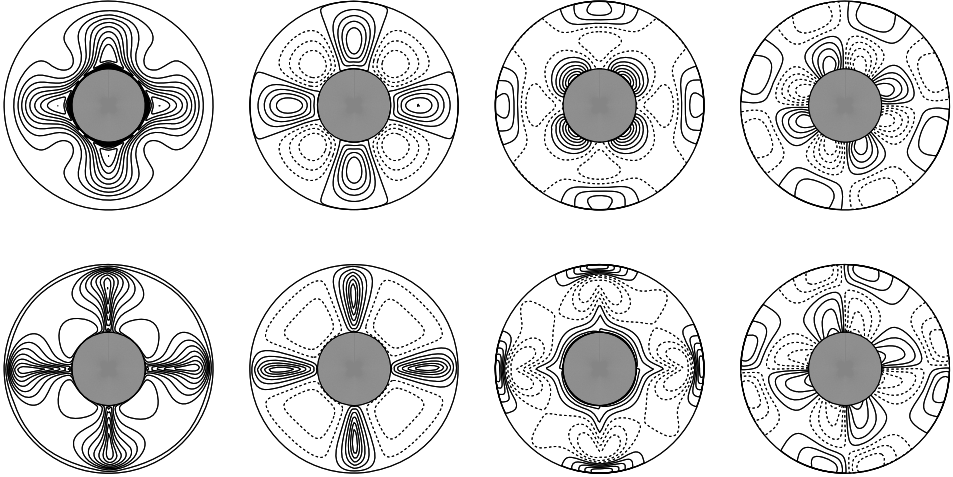


Fig. 2. Equatorial sections of temperature T and velocity field components V_r , V_θ , V_φ (from left to right) for $R_a = 5 \times 10^5$, $E = 10^{-7}$, $P_r = 10^{-5}$ (top) and $P_r = 10^{-3}$ (bottom).

by a circle in Fig. 1). The chosen value of R_a is 5×10^5 , which represents a weakly developed convection for given values of P_r , i.e. close to the onset of convection (represented by the critical Rayleigh number, R_{ac}). The typical space distributions of temperature and velocity are presented in Fig. 2 (equatorial sections) and in Fig. 3 (axi-symmetric meridional sections). The dynamics of thermal convection in rapidly rotating spherical systems is fundamentally different from that in plane-layer systems, i.e. teleconvection and multilayer convective mode are characteristic for convection in rotating spherical systems (Zhang and Schubert, 2000). In our case the convection is not slightly or significantly suppressed in the stably stratified region as it is in the presence of magnetic field (Simkanin, 2008) or if the thickness of stable sublayer is greater than that of unstable one, but it is developed in both sublayers. Figs. 2 and 3 provide a typical example of multilayer convective mode (or structure). Convective motions take place simultaneously in the stable and unstable layers and form a multilayer structure (Zhang and Schubert, 2000). Convective motions concentrate in two separate locations: the Busse-type rolls in the unstably stratified sublayer and the zonal flows in the stably one. This multilayer convective mode is a consequence of the radial stratification, without which they cannot take place (Zhang and Schubert, 2000).

3.2. Prandtl number $P_r = 1$

In the case of $P_r = 1$ the characteristic thermal diffusion time is equal to the characteristic viscous diffusion time ($\tau_\kappa = \tau_\nu$), i.e. thermal and viscous diffusion processes affect the dynamics of convection equally. Dependencies of the monitored output parameters on R_a and E for $P_r = 1$ are given in Fig. 4. E_k and ω increase for given E with a increase of R_a also for $P_r = 1$, but not so rapidly as in the previous case. E_k decreases with a decrease of E . ω also decreases with a decrease of E , except for the interval $R_a \in \langle 5\,000; 50\,000 \rangle$. Our attention was again focused on the case $E = 10^{-7}$ (marked by a circle in Fig. 4). The chosen value of R_a is again 5×10^5 , which represents a developed convection for $P_r = 1$. The typical space distribution of temperature and velocity is presented in Fig. 5 (equatorial sections) and

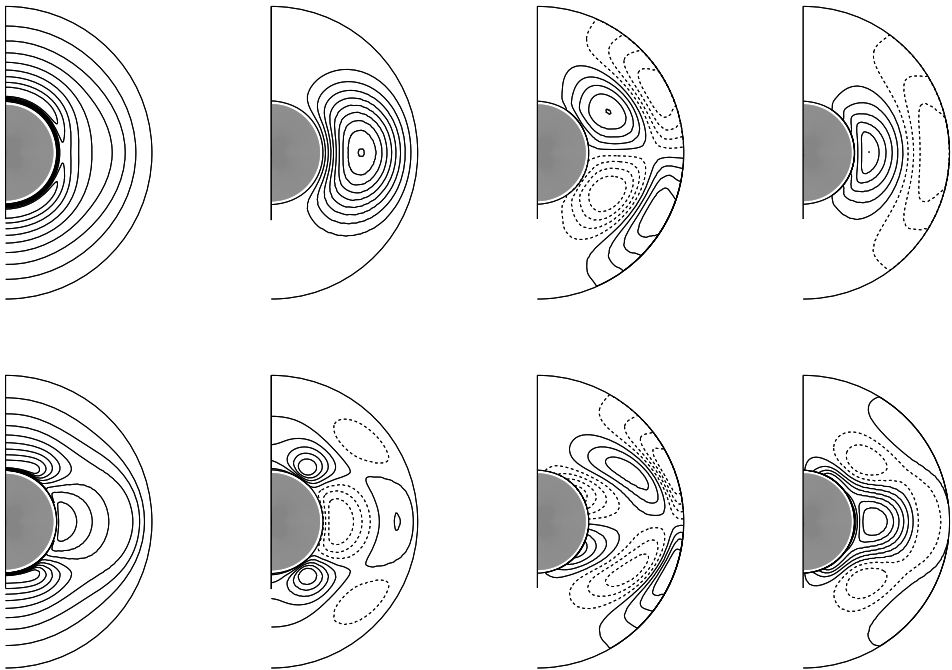


Fig. 3. Axi-symmetric meridional sections of temperature T and velocity field components V_r, V_θ, V_φ (from left to right) for $R_a = 5 \times 10^5, E = 10^{-7}, P_r = 10^{-5}$ (top) and $P_r = 10^{-3}$ (bottom).

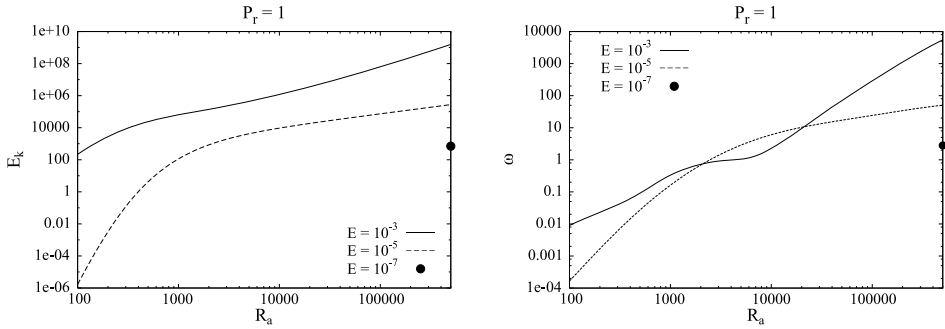


Fig. 4. Dependence of the mean kinetic energy E_k (left) and the mean angular drift frequency ω (right) on the Rayleigh number R_a and the Ekman number E for $P_r = 1$.

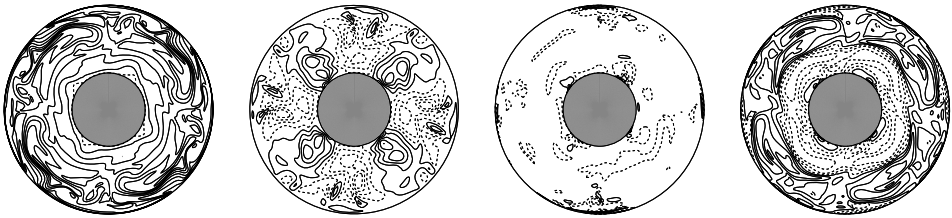


Fig. 5. Equatorial sections of temperature T and velocity field components V_r , V_θ , V_φ (from left to right) for $R_a = 5 \times 10^5$, $E = 10^{-7}$ and $P_r = 1$.

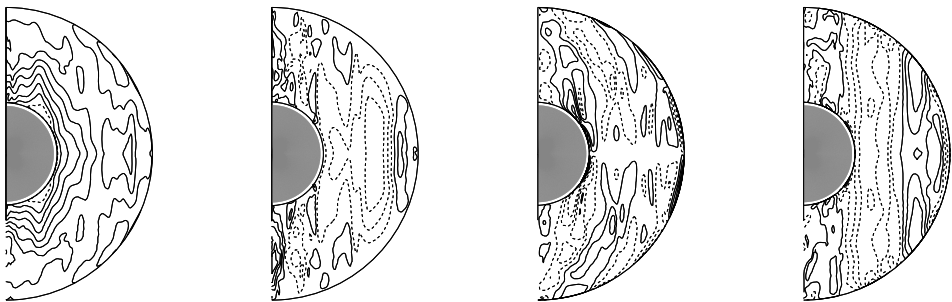


Fig. 6. Axi-symmetric meridional sections of temperature T and velocity field components V_r , V_θ , V_φ (from left to right) for $R_a = 5 \times 10^5$, $E = 10^{-7}$ and $P_r = 1$.

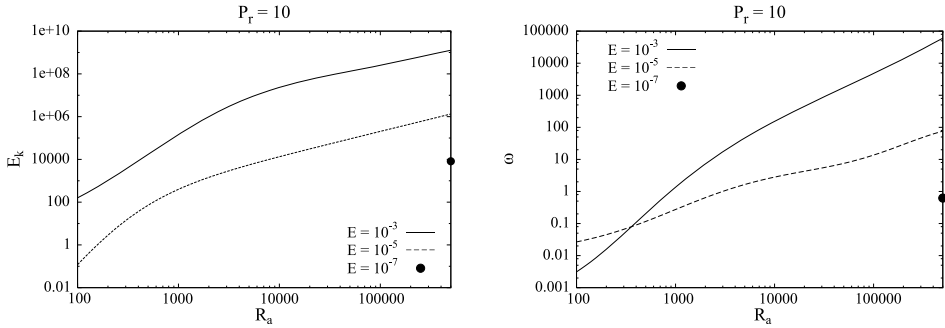


Fig. 7. Dependence of the mean kinetic energy E_k (left) and the mean angular drift frequency ω (right) on the Rayleigh number R_a and the Ekman number E for $P_r = 10$.

in Fig. 6 (axi-symmetric meridional sections). There is a convection developed in both sublayers (not slightly or significantly suppressed in the stably stratified region) and it is possible to observe the small-scale structures (see Figs. 5 and 6). In this case we did not observe any multilayer convection.

3.3. Large Prandtl numbers

In the case of large Prandtl numbers ($P_r > 1$ or $P_r \gg 1$) the characteristic thermal diffusion time is greater (or much greater) than the characteristic viscous diffusion time ($\tau_\kappa > \tau_\nu$ or $\tau_\kappa \gg \tau_\nu$), i.e. viscous diffusion processes dominate over thermal ones. Dependencies of the monitored output parameters on R_a and E for $P_r = 1$ are given in Fig. 7. E_k and ω increase for given E with an increase of R_a for $P_r = 10$ (as in the both previous

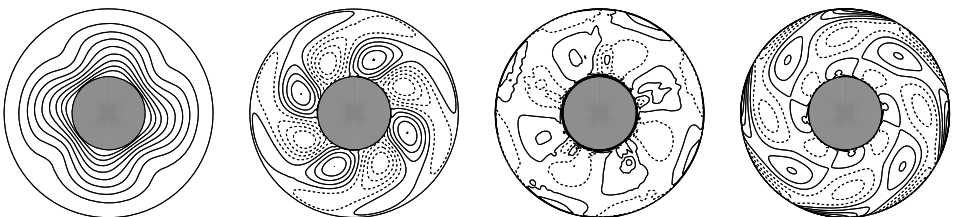


Fig. 8. Equatorial sections of temperature T and velocity field components V_r , V_θ , V_φ (from left to right) for $R_a = 5 \times 10^5$, $E = 10^{-7}$ and $P_r = 10$.

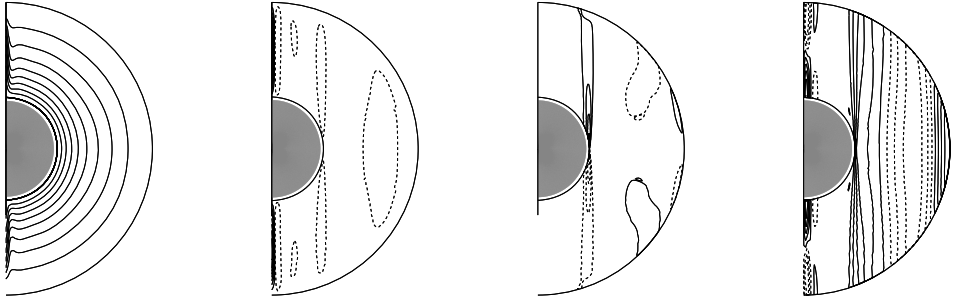


Fig. 9. Axi-symmetric meridional sections of temperature T and velocity field components V_r , V_θ , V_φ (from left to right) for $R_a = 5 \times 10^5$, $E = 10^{-7}$ and $P_r = 10$.

cases). E_k decreases with a decrease of E . ω also decreases with a decrease of E , except for the interval $R_a \in \langle 100; 500 \rangle$. As in the previous cases, our attention was again focused on the value $E = 10^{-7}$ (marked by a circle in Fig. 7). The chosen value of R_a is again 5×10^5 which for given values of P_r represents a developed convection. The typical space distribution of temperature and velocity is presented in Fig. 8 (equatorial sections) and in Fig. 9 (axi-symmetric meridional sections). For large P_r it is possible to observe the convection developed in both sublayers (again not slightly or significantly suppressed in the stably stratified region). Interestingly, the convection tends to be multilayer as in the case of low Prandtl numbers. Looking at Figs. 8 and 9 it is possible to see a development of the multilayer structures.

4. Conclusions

A systematic parameter study of a rotating convection in non-uniformly stratified spherical shells in dependence on Prandtl number, Ekman number and Rayleigh number is presented. Our attention is focused on the case when the thickness of both sublayers (stable and unstable) is the same. Such a case was not investigated in previous studies (Zhang, 1994; Zhang and Schubert, 2000; Šimkanin et al., 2003; Šimkanin et al., 2006; Šimkanin, 2008). Consequently, we place the change of the sign to the middle of the

convective shell. The dynamics of thermal convection in rapidly rotating spherical systems is fundamentally different from that in plane-layer systems, i.e. teleconvection and multilayer convective mode are characteristic for convection in rotating spherical systems (*Zhang and Schubert, 2000*).

In our case, the convection is not slightly or significantly suppressed in the stably stratified region as it is in the presence of magnetic field (*Šimkanin, 2008*) or when the thickness of stable sublayer is greater than that of unstable one, but it is developed in both sublayers. Thus, we conclude that our case (when the thickness of both sublayers is the same) is similar to the case when the thickness of the unstable sublayer is greater than the stable one. The mean kinetic energy and the angular frequency increase for given Ekman number with an increase of the Rayleigh number (except for ω in some small intervals of R_a for $P_r \geq 1$, see 3.2 and 3.3). Both the mean kinetic energy and the angular frequency decrease with a decrease of the Ekman number. These features are well-known. Cases of small and large Prandtl numbers are characterized by creation of multilayer convective structures. Convective motions take place simultaneously in the stable and unstable layers and form a multilayer structure (*Zhang and Schubert, 2000*). Convective motions concentrate in two separate locations: the Busse-type rolls in the unstably stratified sublayer and the zonal flows in the stably one. This multilayer convective mode is a consequence of the radial stratification, without which they cannot take place (*Zhang and Schubert, 2000*). For $P_r < 1$ the convection is weak and for $P_r > 1$ developed. On the other hand, we observed no multilayer convection for $P_r = 1$ if the convection is highly developed. It is possible to observe the small-scale structures.

Our results are in agreement with the previous analyses done in the uniformly (*Busse and Simitev, 2005*) or non-uniformly (*Zhang, 1994; Zhang and Schubert, 2000; Šimkanin et al., 2003; Šimkanin et al., 2006; Šimkanin, 2008*) stratified spherical shells. The convective motions were qualitatively described in *Zhang (1994)*, *Zhang and Schubert (2000)* etc. We showed that the case characterized by the same thicknesses of both sublayers (which was not investigated before) is similar to the case in which the thickness of unstable sublayer is greater than that of stable one.

Acknowledgments. This research has been supported by the Grant Agency of the Academy of Sciences of the Czech Republic (Grant No. IAA300120704) and the John von Neumann Institut für Computing, Forschungszentrum Jülich (Grant k2720000). We

would like to thank the Institute of Physics of Academy of Sciences of CR, Prague for CPU time on the Sun Grid Engine (the Luna project).

References

- Busse F. H., Simitev R., 2005: Convection in rotating spherical fluid shells and its dynamo states. In: Soward A. M., Jones C. A., Hughes D. W., Weiss N. O. (Eds.), *Fluid Dynamics and Dynamos in Astrophysics and Geophysics*, CRC Press, New York, USA, 359–392.
- Christensen U. R., Aubert J., Cardin P., Dormy E., Gibbons S., Glatzmaier G. A., Grote E., Honkura Y., Jones C., Kono M., Matsushima M., Sakuraba A., Takahashi F., Tilgner A., Wicht J., Zhang K., 2001: A numerical dynamo benchmark. *Phys. Earth Planet. Inter.*, **128**, 25–34.
- Christensen U. R., 2006: A deep dynamo generating Mercury’s magnetic field. *Nature*, **444**, 1056–1058, doi: 10.1038/nature 05342.
- Fearn D. R., Loper D. E., 1981: Compositional convection and stratification of the Earth’s core. *Nature*, **289**, 393–394.
- Guba P., Worster M. G., 2006: Nonlinear oscillatory convection in mushy layers. *J. Fluid Mech.*, **553**, 419–443.
- Harder H., Hansen U., 2005: A finite-volume solution method for thermal convection and dynamo problems in spherical shells. *Geophys. J. Int.*, **161**, 522–532.
- Hejda P., Reshetnyak M., 2003: Control volume method for the dynamo problem in the sphere with free rotating inner core. *Stud. Geophys. Geod.*, **47**, 147–159.
- Hejda P., Reshetnyak M., 2004: Control volume method for the thermal convection problem in a rotating spherical shell: test on the benchmark solution. *Stud. Geophys. Geod.*, **48**, 741–746.
- Jones C. A., 2000: Convection-driven geodynamo models. *Phil. Trans. R. Soc. Lond.*, **A 358**, 873–897.
- Patankar S. V., 1980: *Numerical heat transfer and fluid flow*. Taylor and Francis, New York, USA.
- Reshetnyak M., Steffen B., 2005: A dynamo model in a spherical shell. *Numerical methods and programming*, **6**, 27–34.
- Roberts P. H., Glatzmaier G. A., 2000: Geodynamo theory and simulations. *Rev. Mod. Phys.*, **72**, 4, 1081–1123.
- Stanley S., Bloxham J., 2004: Convective-region geometry as the cause of Uranus’ and Neptune’s unusual magnetic fields. *Nature*, **428**, 151–153.
- Stanley S., Bloxham J., 2006: Numerical dynamo models of Uranus’ and Neptune’s magnetic fields. *Icarus*, **184**, 556–572.
- Šimkanin J., Brestenský J., Ševčík S., 2003: Problem of the rotating magnetoconvection in variously stratified fluid layer revisited. *Stud. Geophys. Geod.*, **47**, 827–845.

-
- Šimkanin J., Brestenský J., Ševčík S., 2006: On hydromagnetic instabilities and the mean electromotive force in a non-uniformly stratified Earth's core affected by viscosity. *Stud. Geophys. Geod.*, **50**, 645–661.
- Šimkanin J., 2008: Control volume method for hydromagnetic dynamos in non-uniformly stratified spherical shells. *Contr. Geophys. Geod.*, **38**, 1, 1–15.
- Šimkanin J., Hejda P., 2009: Control volume method for hydromagnetic dynamos in rotating spherical shells: testing the code against the numerical dynamo benchmark. *Stud. Geophys. Geod.*, **53**, 99–110.
- Zhang K., 1994: On coupling between the Poincare equation and the heat-equation. *J. Fluid Mech*, **268**, 211–229.
- Zhang K., Schubert G., 2000: Teleconvection: remotely driven thermal convection in rotating stratified spherical layers. *Science*, **290**, 1944–1947.